Velocity Analysis for Depth Conversion: A Case Study of Block A, Baga/Lake Sub-basin in the Borno Basin, Northeastern Nigeria

[1]Omolaiye, G.E, [2]Saminu, O., [3]Ajadi, J. and [3]Jimoh, A.Y.,

[1]Geoslice Solution Limited, Lagos Nigeria.
[2]Department of Geophysics, University of Ilorin, Nigeria
[3]Department of Geology and Mineral Science, Kwara State University, Malete, Nigeria

ABSTRACT

Time-depth conversion analysis of time migrated seismic images was undertaken on Block A, Baga/Lake sub-basin of Borno basin Nigeria, to predict the appropriate velocity model suitable for depth conversion away from six existing well control points. Three velocity models were used for the time to depth conversion including average velocity-time analytical function, 2nd Order Polynomial time- depth analytical function and instantaneous velocity analytical function. The velocity models were tested with the shallow and deep horizons representing the tops of Kerri-Kerri and Gongila Formations penetrated by six wells fairly spread on the 3,891 km^2 of 3D seismic data. The results show that each model has variable degree of accuracy after depth conversion at the two formation tops. The average velocity-time analytical technique appeared as the best technique for the time-depth conversion having errors in the range of -0.12 to 145 meters at shallow and deeper formation respectively. The 2nd order polynomial time-depth analytical function and V_0-K techniques gave a depth uncertainty greater than 135 meters at the shallow formation and over 1,000 meters at the deeper formation. The maximum percentage error recorded for both formations using average velocity technique was 0.48% this is less than 5% considered good in the practical situation, it is therefore recommended to be used for velocity modeling and depth conversion study in Baga/Lake sub-basin of Borno Basin, Northeastern Nigeria.

Keywords: Seismic Image, Depth Conversion, Velocity Analysis, Borno Basin, Chad Basin.

GALLEY PROOF

INTRODUCTION

Seismic reflection data depict the subsurface in recorded two-way time. Most seismic data are interpreted in the time domain, which is fast and adequate for various situations (Etris *et al*., 2002). Time domain analysis of stratigraphic features such as seismic facies, sequence stratigraphic analyses are better when converted to corresponding depth. This is because the result of the analysis in most cases is the same with varying structure. The interpretations, however become a bit dicey when undertaking structural interpretation based on an assumption

of constant velocity model which may be wrong in real situation. Sometimes, a compact area of high velocity sediment/rock can cover-up in the time domain as a consistently deposited stratum of sediments covering a structural high interpretation, also a simple geology can give rise to false highs or can vague the true highs in the interpretation (Etris et al 2002). Overburden can obscure structures, besides a robust time-depth function can delineate conceals structures thereby illuminating possible detoured reserves. A good seismic image with good well-ties and a consistent time-depth function is vital in interpretation for both exploration and field development.

In spite of the substantial improvements in seismic acquisition in recent years, depth conversion remains a vita means of converting a seismic record into true geologic depth and for risk valuation and ambiguity analysis (Velasquez and Alfonso, 2018). It also a means of eliminating the structural vagueness intrinsic in time and validate structure. Therefore, it is essential for explorationists to substantiate structures in order to be sure of the existence of a drillable trap (structural) when preparing for an exploration well, to estimate the gross thickness of a prospects and determine the spill point in order to estimate the petroleum economics, or to delineate evaded structural highs to drill with infill wells (Velasquez and Alfonso, 2018).

Several techniques of time - depth conversion have been used and published by researchers. Analytical velocity functions (Marsden et. al 1995), V_0–K method of depth conversion (Marsden 1992), Velocity analysis using wave equation (Sava and Biondi, 2004), Velocity trends analysis (Omolaiye et al. 2011), Various velocity techniques for Depth-conversion (Velásquez1 and Alfonso, 2018), Seismic velocities for depth conversion (Carter, M. D., 1989, Krehbiel, 1993, Keho and Samsu 2002, Al-Chalabi, 1994, Al-Chalabi, M., 1997, Schultz, 1999, Al-Chalabi, M., 2014). This study adopted three different methods of depth conversion namely; (i) 2nd Order Polynomial time-depth analytical function, (ii) average velocity-time analytical function and (iii) instantaneous velocity analytical function in the study area. The resultant residual values were compared to determine the appropriate velocity depth conversion methodology used for the study area.

Geology and Structural Framework of the Baga/Lake Area

The Chad basin is one of the largest basins in Central African region. This intra-cratonic basin has geographical spread and extent across Nigeria, Chad, Niger Republic, Cameroun and Central African Republic, an area that remain relatively inactive geologically over a long period. The

tectonic history of Chad basin passed through five stages, from the Pan African orogeny to the present (Figure 1). This suggests that the basin is a component of West African Rift System (WAS), which led to breaking away of the African continent in the Early Cretaceous, is extensional in characteristics with thick continental to marine clastics sediments and minor volcanics (Genik, 1992). Thick deposit of mainly siliciclastic sedimentary layers, in addition to the unearthing of commercial quantity of hydrocarbon in adjoining countries within the basin, heightens exploration interest in the Nigerian sectors.

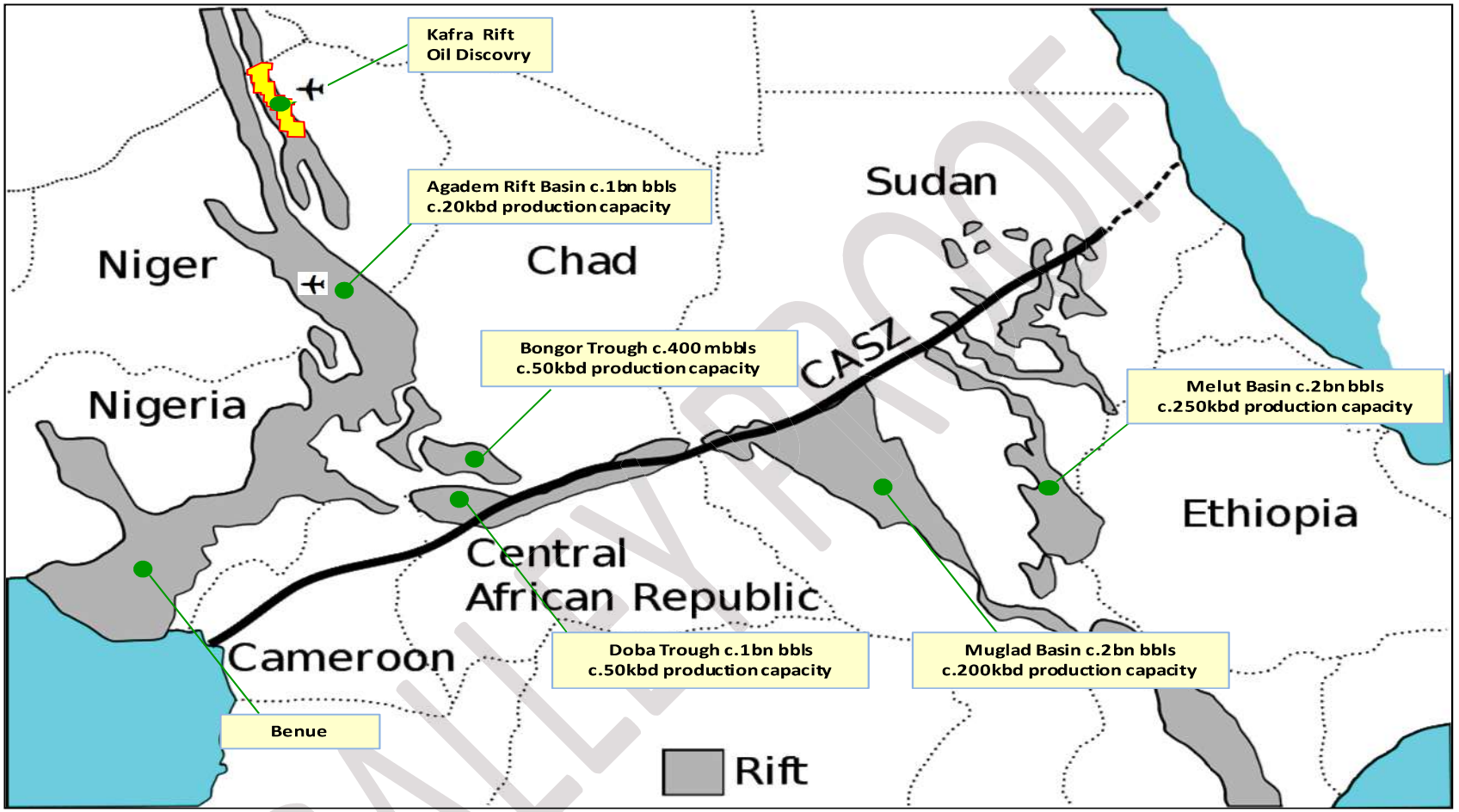


Figure 1: Map of Chad and its neighboring basins (Genik 1993).

GALLEY PROOF

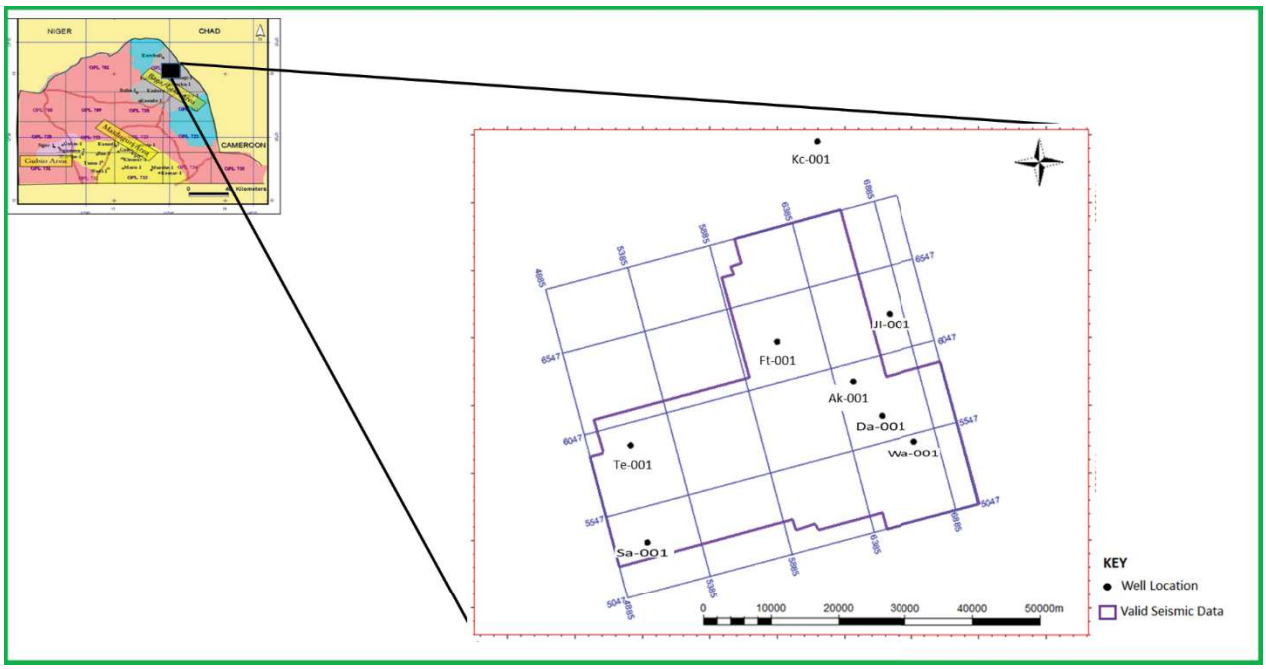


Figure 2: 3D Seismic Basemap showing Block A, Baga sub-basin in Borno Basin

The study area is situated in the Lake/Baga sub-basin in the NE of the Borno basin (Figure 1). It covers an area of about 3,891km^2 with altitude of around 300 m within the lake area (Figure 2). The two major fault type encountered in Baga/Lake sub basin are (1) Deep sited synthetic faults with significant throw that affects both the basement and the overlying sediments and (2) some antithetic faults restricted to the sediments (Avbovbo, 1986). The synthetic faults are more dominant and define the west and the eastern limit of the depocenter, separating the study area into two different compartments. The antithetic faults are possibly developed as relief faults in responseto variations in stress within the system. Most of the faults in the Baga/Lake sub-basin terminate below the regional angular unconformity that separates Cretaceous from Tertiary sedimentation (Figure 3).

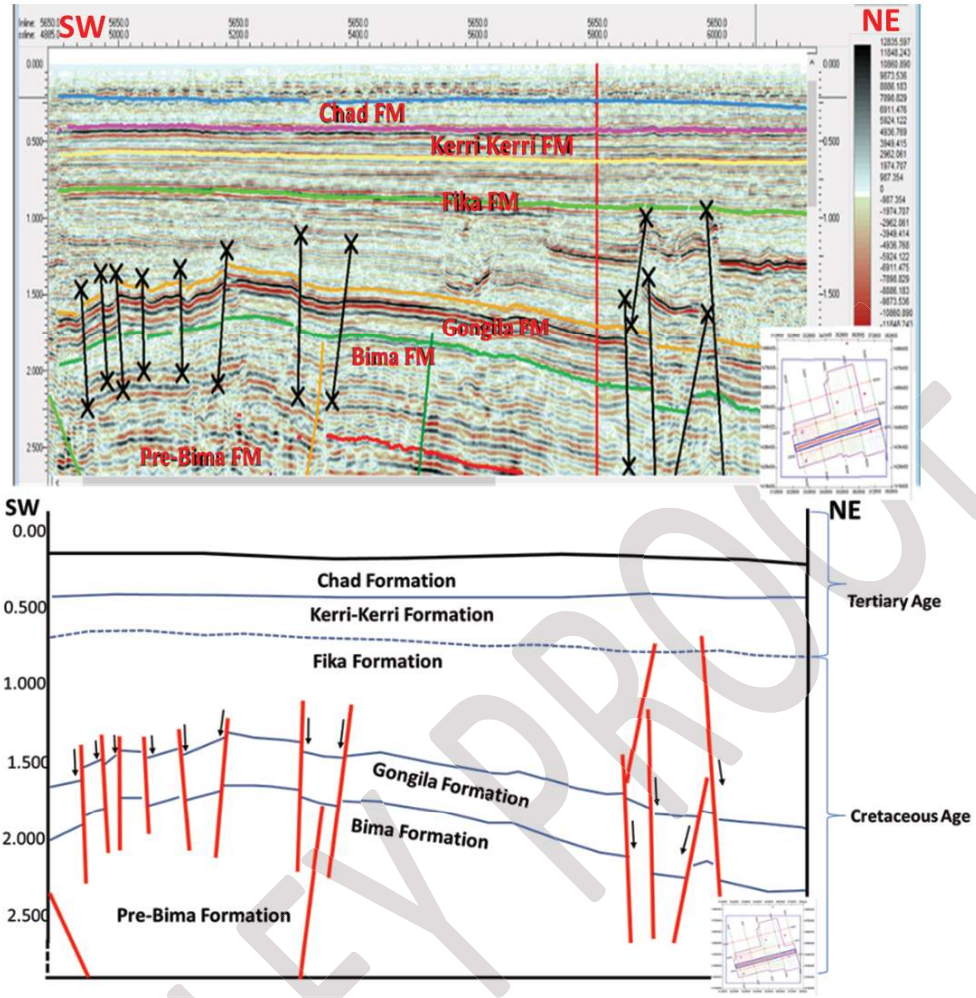


Figure 3: A NE-SW seismic section Baga/Lake area showing the interpretation

1.2 Stratigraphic Setting of the Borno Basin

The Borno basin consists of marine to fluviatile/deltaic sediments. The stratigraphic framework of the basin comprises of the following units from top to bottom: the Chad, Kerri-Kerri, Gombe, Fika, Gongila, Bima and Pre-Bima Formations (Avbovbo et al 1986).

1.2.1 The Pre-Bima Formation

The Pre-Bima sediments is the basal formation in the Borno basin and directly overlie uncomfortably on the crystalline basement rocks (Guiraud 1990, 1991 and Genik 1992). The group encompasses three subdivision, namely; Upper, Middle and Lower Bima sandstones.

GALLEY PROOF

1.2.2 *The Bima Formation*

Sedimentation is thought to have commenced during the Albian with the deposition of continental feldspathic sandstones that is poorly sorted, sparsely fossiliferous and medium to coarse-grained referred to as the Bima Sandstone of Albian-Cenomanian age. The formation varies with thickness of 3050m. Conglomeratic to fluviatile/deltaic sediments are common and the various lithofacies seen indicates widely varying environments of deposition (Adekoya et al 2014, Ola et al 2017). This Formation unconformably overlies the pre-Bima Formation.

1.2.3 The Gongila Formation

This formation is made up of alternation of shale and sandstones sequence with fossiliferous limestone beds deposited in a shallow-marine environment. This lithologic unit is an intermediate between the Bima Sandstones (purely continental) and the Fika unit (marine Shales). It generally begins with a basal limestone unit. A Turonian age is attributed to this formation and it overlies Bima Formation. The average thickness of the formation is 420 m (Olugbenro et al 1997 and Genik 1993).

1.2.4 The Fika Formation

The peak marine transgression occurred during the Campanian to Santonian age with the deposition of the Fika Shales which are bluish-black, open marine shales, rich in ammonite with average thickness of about 430 meters. There is an occurrence of intercalation of thin limestone beds within the shales and siltstones (Obaje et al.2004a, Okosun 1995).

1.2.5 Gombe Formation

This formation is deposited in estuarine to deltaic environments. . It is a regressive sequence of siltstone, sandstone and clay. There is an occurrence of coal beds within the sequence, the formation overlain the Fika shale at the center of the basin, hence; it is completely eroded in most of the wells in the Baga/Lake sub-basin. Moumouni et al. (2007) reported in their study that this formation is missing in Albarka-1, Kasade-1, Kanadi-1 and Gaibu-1 wells. The formation is well bedded to cross-bedded and are dated Maastrichtian. The average thickness of the formation is about 350m. Then, general uplift occurred with widespread erosion of the above-described formations, at the end of the Cretaceous.

1.2.6 *Kerri-Kerri and Chad Formations*

These Formations are Tertiary/Quaternary and rest unconformably on the Cretaceous sediments. They may reach a total thickness of 800m and are generally flat-lying. They are made up of

alternating layers of sandstones and conglomerates with well-developed cross-bedding, indicating a deltaic environment. The more clayey nature of the sandstones and siltstones suggest more lacustrine environments (Adegoke et al.1986, Onuoha, 1999).

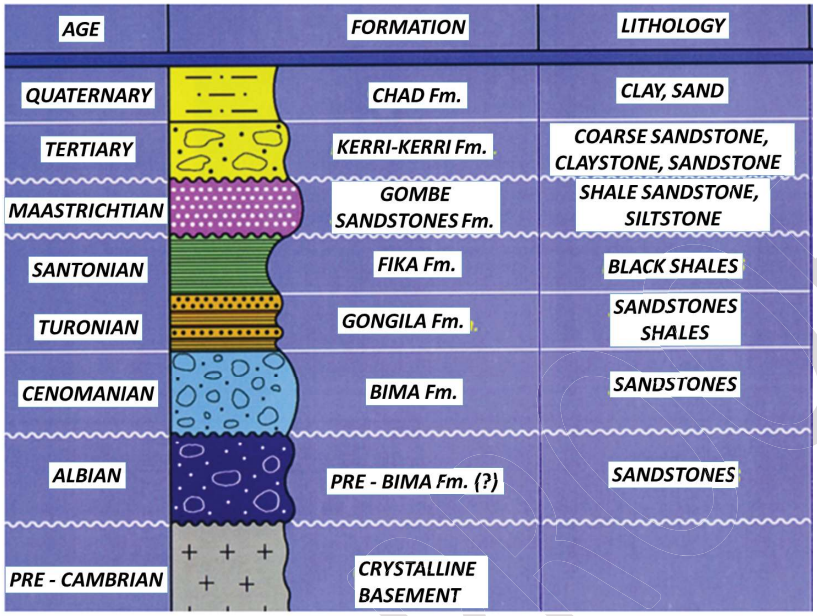


Figure 4: Lithostratigraphy overview of Chad Basin (After Avbovbo et al 1986)

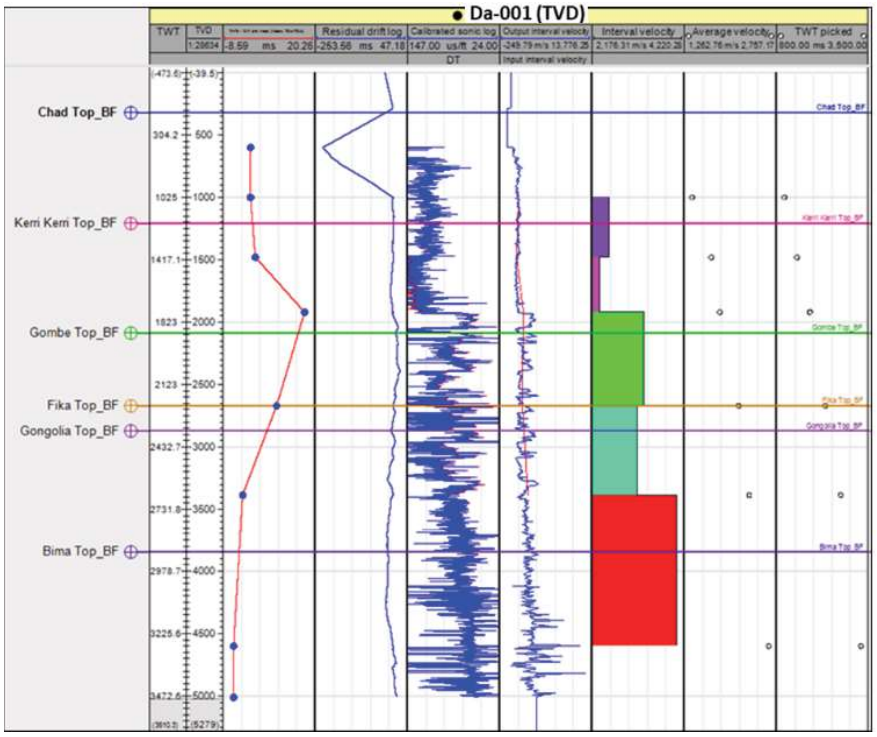
2.0 Materials and Methods

A 3,891 km^{2}of 3D seismic data acquired in 1997 with bin size 25m x 25m was used in this study. The interpretation was done using full stack time migrated data. The quality of the seismic data is good and synthetic seismograms of six wells were generated to establish seismic to well tie. First, a sonic data calibration with respect to available checkshot data was employed as quality control (QC) method for data consistency and check for invalid velocity information. It was observed that velocity information followed expected trends with no abnormal velocity variation detected. Then a reflectivity co-efficient log was generated and convolved with a synthetic wavelet to obtain a synthetic seismogram for each well. The synthetic seismogram was then compared with a set of traces around the wellbore and degree of correlation examined. No bulk time shift was applied in any of the wells to avoid distorting the velocity information as validated from the initial checkshot data. A sample of the sonic data calibration, synthetic seismogram generation and seismic-well tie process for two wells are shown in Figure5.

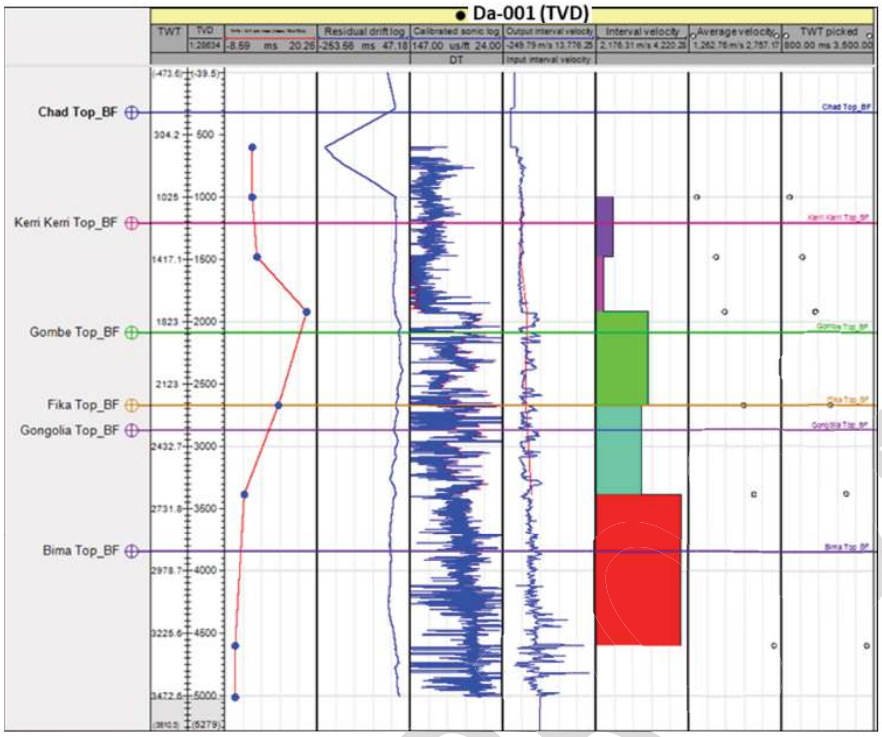
GALLEY PROOF

The calibrated velocity log computed in the well tie process ensured the well velocity data derived time-depth values tied the seismic data. With a good well to seismic tie, the top of the formations as picked from well data were extrapolated and mapped across the entire seismic coverage Figures 6 and 7.

Five horizons corresponding to the top of the formation (Chad, Kerri-Kerri, Fika, Gongila and Bima) were interpreted (Figure 3). Time structure maps for the interpreted levels were then obtained using simple-kriging method with boundary limits defined by the interpretation grid and associated fault polygons. The different depth conversion methods: average velocity-time analytical function, 2nd order polynomial time-depth analytical function and instantaneous velocity analytical function were tested and used to convert time maps to depth domain. This is done to ensure that the best conversion model was chosen as depth maps obtained often change with respect to the conversion model used. Final chosen model would be based on that method which gives the least residual after the conversion process.



a



b

Figure 5a and 5b: Sonic log to Checkshot data calibration for Da-001 and Te-001 wells

GALLEY PROOF

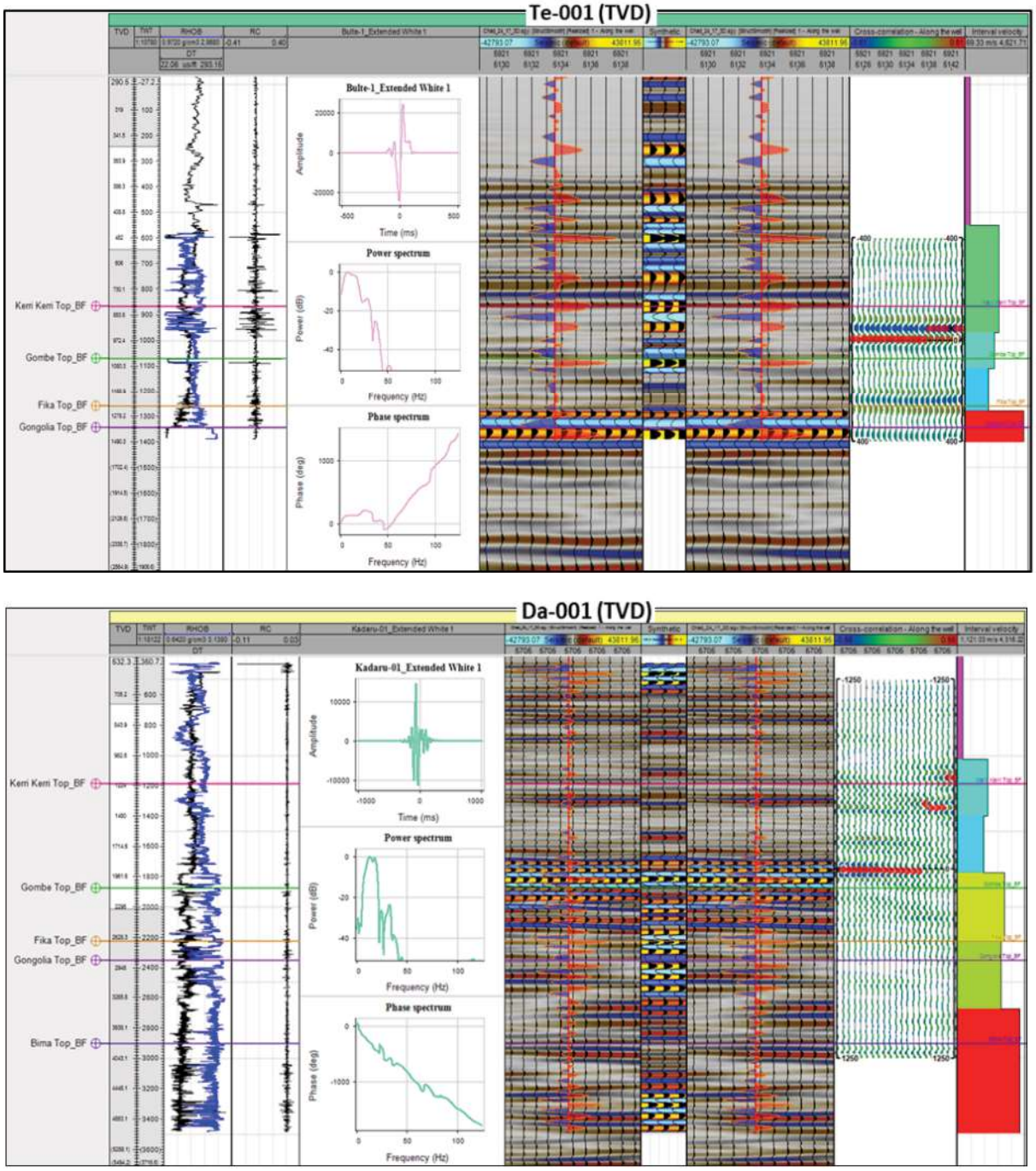


Figure 6a and 6b: Synthetic seismogram generation and Seismic to well tie process panel for Te-001 and Da-001 wells

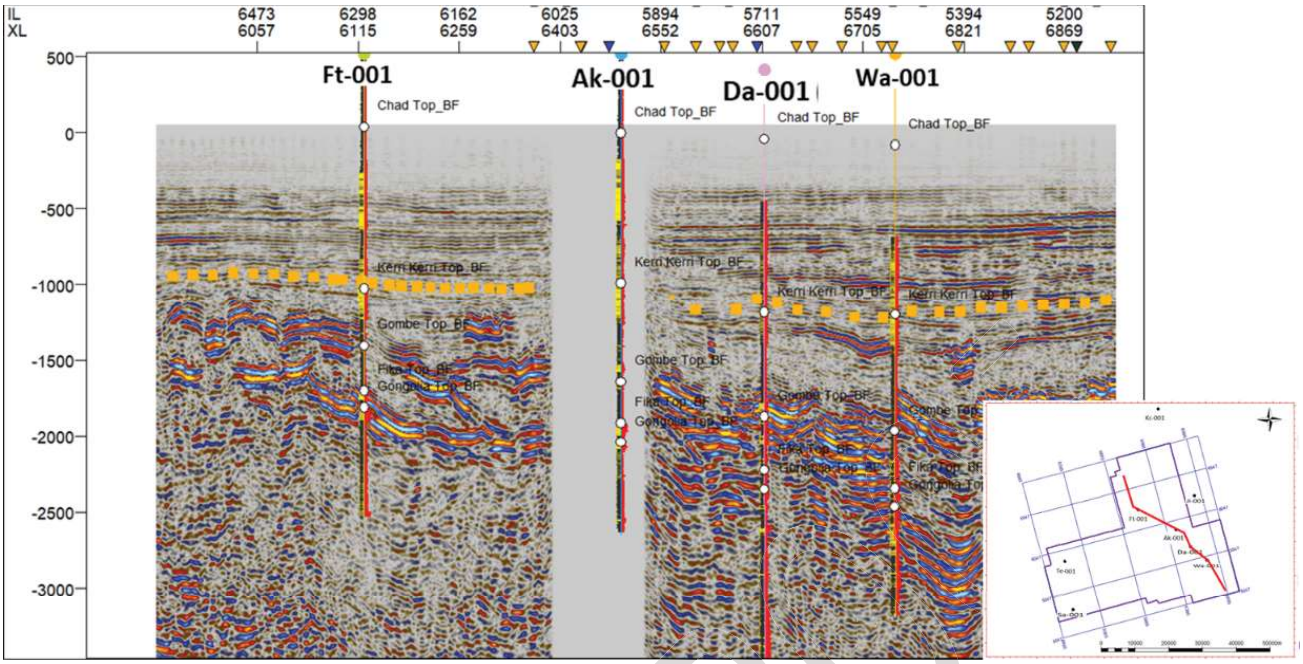


Figure 7: Seismo-Well tie Arb-line validating correlation between Ft-001, Ak-001, Da-001 and Wa-001 wells.

2.1 Depth Conversion

A multi-layer velocity depth conversion approach was used, the study area was divided into separate formations (Chad, Kerri-Kerri, Fika, Gongila and Bima) as defined by the biostratigraphy study. Each formation with different, but consistent, velocity-depth function. For each formation, discrete velocity function was developed. This led to depth forecast for the formation base, given the formation top from the preceding computation. E.g. Chad Formation top was defined as the datum, then Chad Formation base becomes Kerri-Kerri Formation top and this process is repeated to the last formation (Bima Formation) the last interpreted formation. These formations may have substantial velocity variation because they form the overburden above the region of concern (Figure 8).

GALLEY PRO

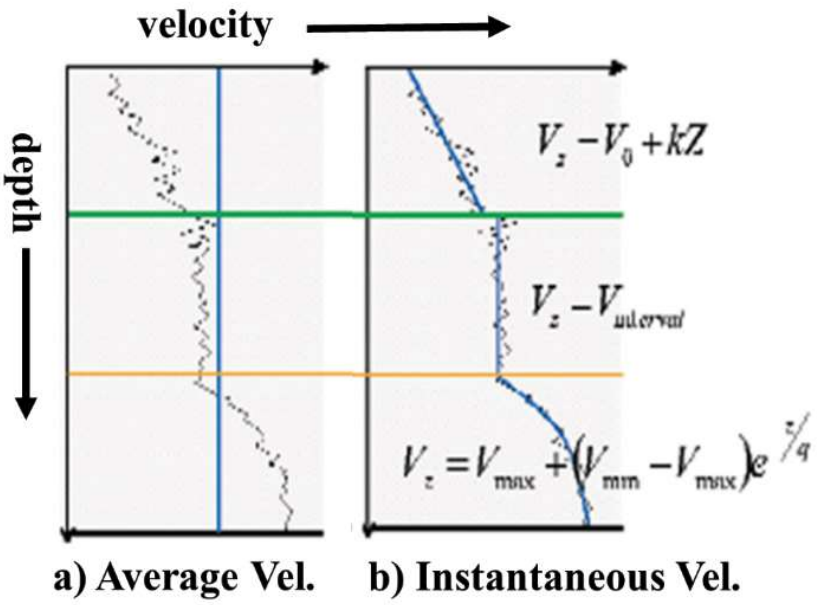


Figure 8: Typical velocity model built for each layer

2.2 Velocities: Basic definitions

Velocity is a vector quantity that relate distance and traveltime along a ray path ($V(\tau) = (V_x, V_y, V_z)$ and determination of optimum model $V(\tau)$ is very important in seismic imaging, processing and depth conversion. Mathematically, rock layers can be analyzed based on the seismic velocities illustrated from geologic model (Amery 1993). Layers with distinct velocities confined by flat planes are the simplest resolvable model (Figure 9). Each layer with constant velocity (*V),* a traveltime (Δt) and a thickness (Δh) straight up through the layer, henceforth $\Delta h = V\Delta t$.

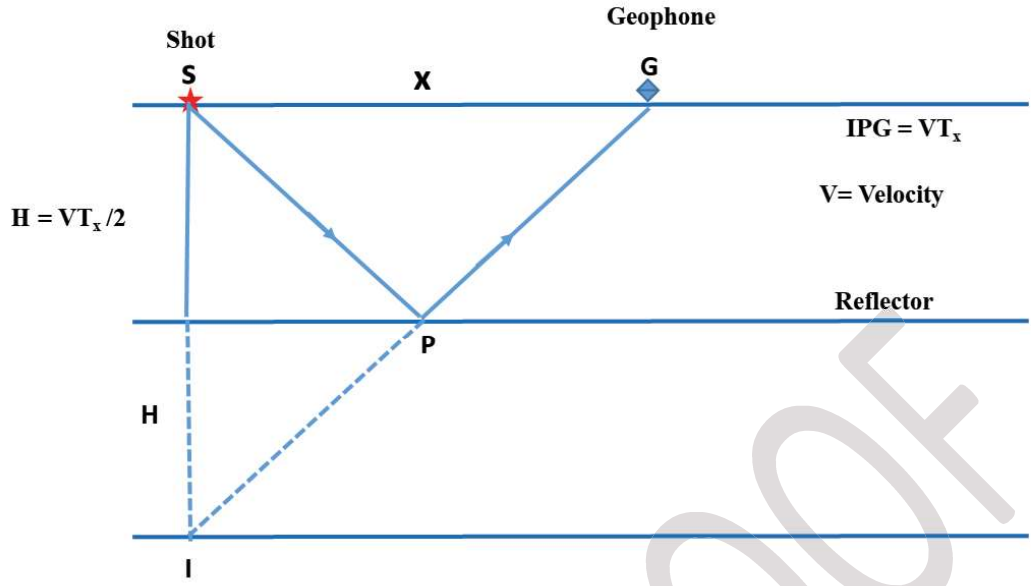


Figure 9: A Single layer geologic model and plane reflector

Seismic velocity variation with depth is a vital facet of seismic study and analytic expressions had been established over time to define the variation. The most extensively used ***instantaneous velocity*** as a direct relationship with depth (Al-Chalabi, 1997b, Slotnick, 1936).

$$V_z = \frac{dz}{dt} = V_0 + kZ \qquad 1$$

where $V_{z=}$ instantaneous velocity @ depth Z, V_0 = intercept @ Z=0 and k= gradient.

Interval Velocities is the speed of broadcast of seismic waves in the vertical direction within a particular interval. It uses constant velocities for each layer, this vertical velocity are measured directly from zero offset VSP, Checkshot and well logs.

$$V_{int} = \frac{\Delta z}{\Delta t} \qquad 2$$

where V_{int} is the Interval velocity, Δz change in depth and Δt change in time.

A*verage velocity (*V_{avg} is the velocity measured by lowering of a detector (geophone) into the wellbore through a cable while a shot is detonated close to the surface. The traveltime of energy transmitted from the source to the geophone are measured (Figure 10). The depth to the detector below the shot divided by the computed traveltime is equivalent to the average velocity of wave transmission from the shot to the detector (Amery, 1993).

GALLEY PROOF

$$V_{avg} = \frac{\sum_{i=1}^{n} V_i \Delta t_i}{\sum_{i-1}^{n} \Delta t_i} \quad (3)$$

Information about structural shape of the subsurface can be obtained from wave propagation and seismically derived velocities, when properly applied with diverse approaches, gives several models that are useful for depth conversion.

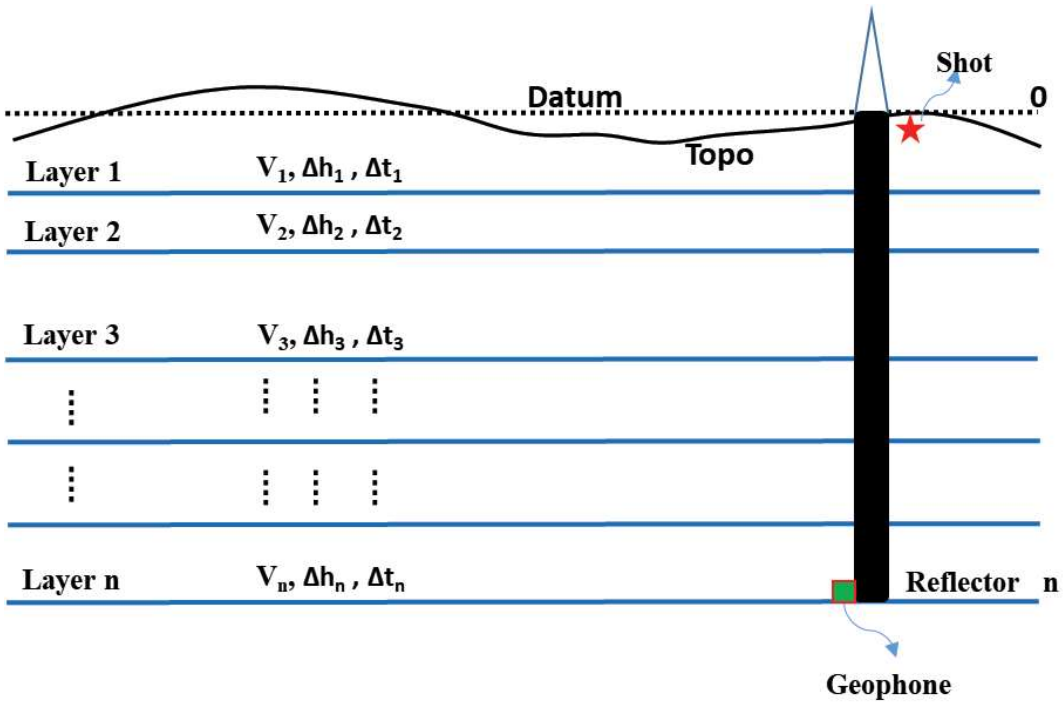


Figure 10: A typical well velocity survey measuring $\mathbf{V_{avg}}$ in a plain layered earth model

2.21 Average Velocity-Time Analytical Function

This process involved the generation of average velocity maps for each individual interpreted horizon after the seismic-well tie process. The average maps are obtained from a simple grid of average velocity values calculated at well locations based on the time-depth relationship (TDR) of time grids (in time) and related well tops (in depth). Thereafter, a depth map for a corresponding time grid is obtained by simple multiplication with average velocity maps generated across the area of interest. The initial depth maps obtained from this process is also finally flexed to well data and residuals obtained documented. Smoothing operation was not performed on any of the velocity maps generated and used in this study.

2.22 2nd Order Polynomial Time- Depth Analytical Function

This process involved making a crossplot of time versus depth values obtained from checkshot data available for wells within the area. Considering these points as subsets of the regional velocity distribution of the area, they were then grouped and a polynomial line of best fit was made for the points and equation of best fit used to transform the time maps into depth maps. This initial depth map generated is then stretched to the well depth point and the residual values of fit at each well location are recorded.

2.23 Instantaneous Velocity Analytical Function

This technique V_0k+Z (abbreviated to V_0k) is valid when a linear relationship between instantaneous velocity and depth is documented (Syukri et al 2014). The rise in velocity with respect to depth due to compaction is a quantifiable and a vital predictive tool for depth conversion. The technique involves isolation of velocity layers related with lithologies displaying well defined instantaneous velocity-depth trends (Marsden 1992). As the solution of the equation in time results in an exponential term, the V_0k methodology is more complex in terms of calculations compared with the polynomial time-depth technique though, they both uses the same velocity data. A depth map is then obtained by a multiplication of the time map with similar velocity grid values obtained from the velocity cube. Resulting maps for this scenario are also moved to well tops with residual values documented.

3.0 Results and Discussions

3.1 Results

The three methods of velocity model tested for the conversion of tops of Kerri-Kerri and Gongila Formations representing the shallow and deep formations in this study are: (1) average velocity-time analytical function, (2) 2nd Order Polynomial time-depth analytical function and (3) instantaneous velocity analytical function. The reliability of velocity model depends on the use of appropriate detailed velocities, consistent with the geology and integrates all existing velocity evidence, weighting different types (wells and seismic) properly.

3.1.1 Average Velocity-Time Analytical Function

Two average velocity maps were generated and used for the depth conversion using this technique. Generally, we have average velocity increase from the west to the east in the two

GALEY PROOF

maps (Figure 11). For Kerri-Kerri average velocity map, the least average velocity of 1,240m/s was observed around Te-001 and Sa-001 wells at the south western section and there is gradual increase towards the east and peaked at about 1,640m/s near Wa-001 well at the south eastern part of the block. The Gongila average velocity map also follow the same velocity variation pattern with average velocity of about 1,560m/s at the south western part and about 2,240m/s south eastern part of the block.

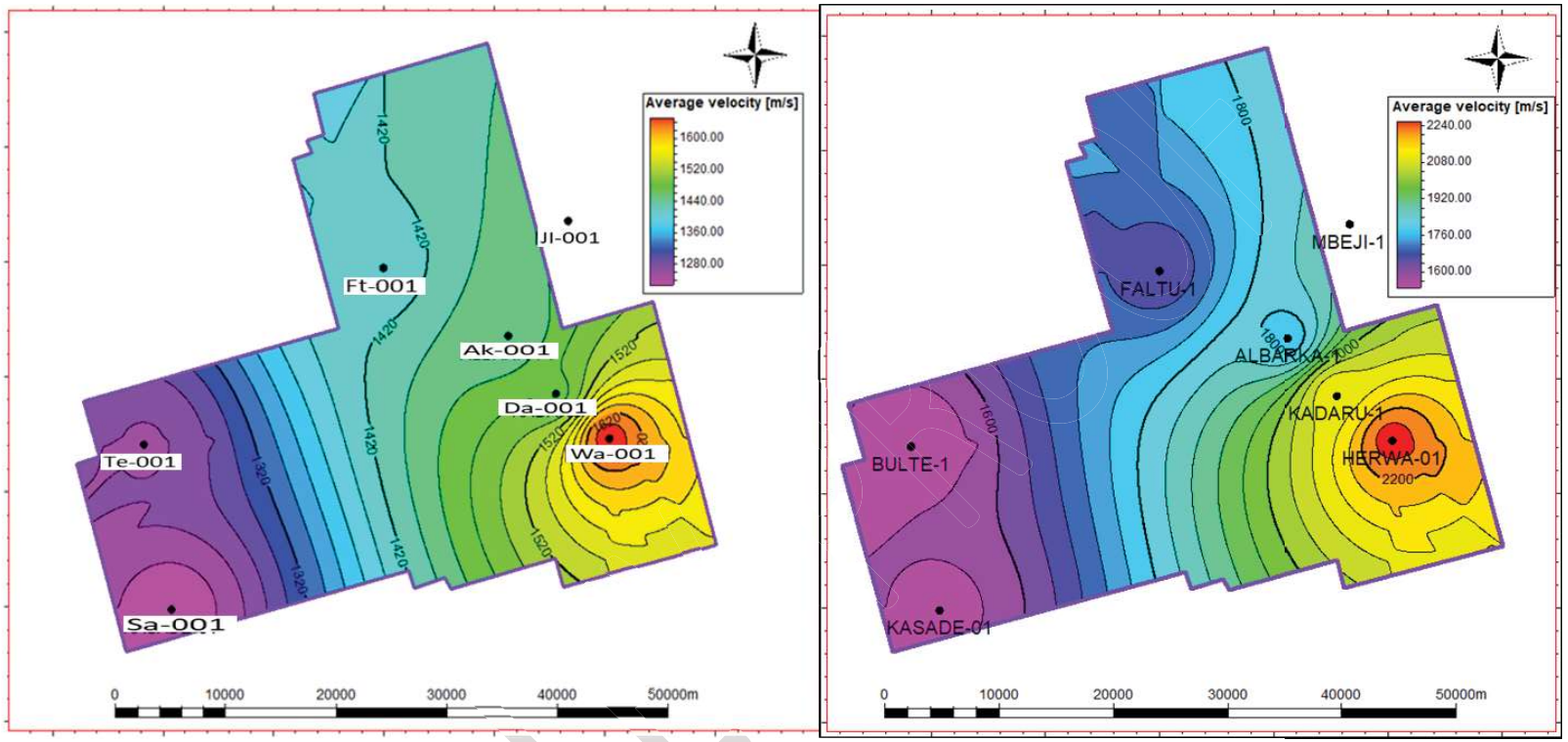


Figure 11a and 11b: Average Velocity maps generated over the Kerri-Kerri and Gongila Formation Tops horizon

GALLEY PROOF

3.1.2 2nd Order Polynomial Time- Depth Analytical Function

The time-depth curve relation generated from the line of best-fit of checkshot data shows a distinctive compaction trend of time-depth function. The best-fit parameters are suited quite well at the shallow formations and fairly suited at deeper level to check-shotdata. The line of best-fit obtained is a polynomial function with the corresponding equation derived for depth conversion in the study area is stated below with covariance value of 746625.

$$Y = 300.205 + 0.76169X - 0.00020746X^2 \quad 4$$

Where: Y is the depth and X is the two-way reflection time from the surface to the base of the layer.

The resulted depth structure map is a vertical conversion from time to depth, the average high residual obtained after depth conversion using this method could be associated with the scattered data points around the line of best-fit lines (Figure 12). The geologic factors responsible for the scatter are: tectonic history, varying lithology (fluctuation in sand/shale/limestone ratios) and pressure regimes. Lower errors were obtained where the line of best-fit lie exactly on the data points which become higher at the deeper level because the data are not precisely on the line of best fit. Hence, the average errors generated after depth conversion increases from -250m at the shallower horizon (Kerri-Kerri Formation) to approximately 1,516m in Gongila Formation representing the deep horizons (Table 2).

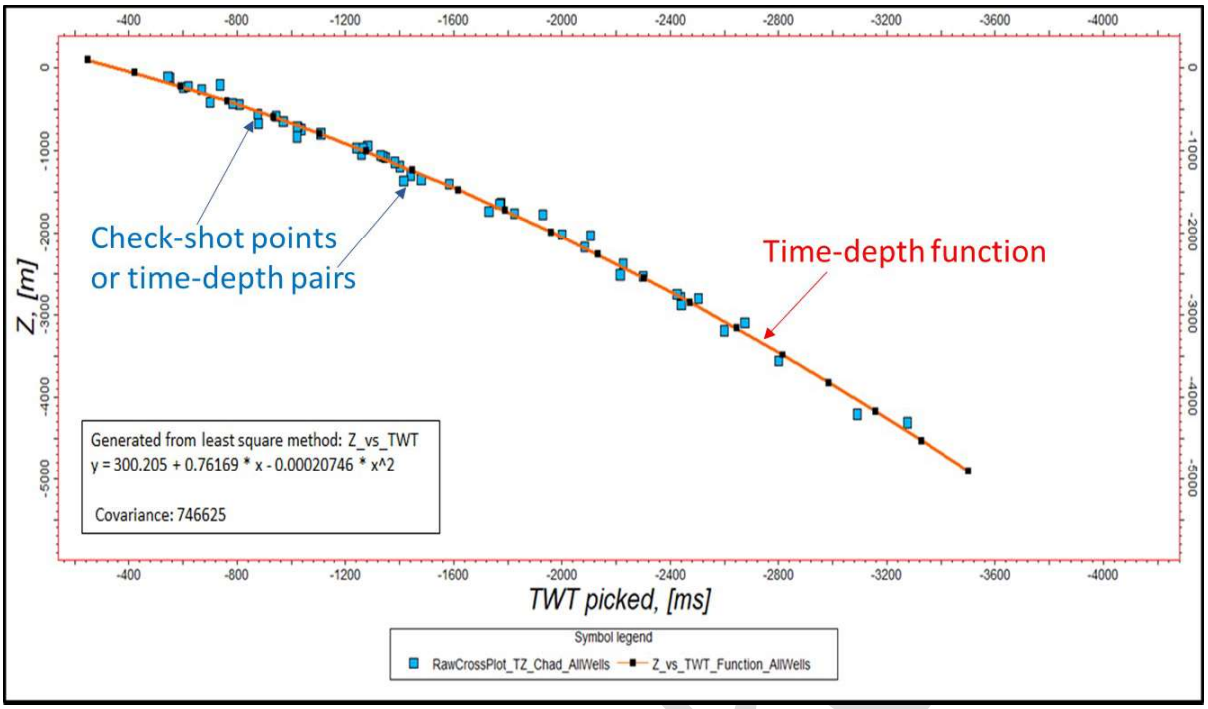


Figure 12: Polynomial function line of best fit and corresponding equation to be used in depth conversion.

3.1.3 Instantaneous Velocity Analytical Function

Marsden 1992 state that if instantaneous velocity increase linearly with depth, then V_0k+Z technique can be used in any formation where the velocity log shows a linear increase with depth. In this study area, the high errors obtained using this method in depth conversion could be as a result of portion of the formation with velocity not increasing linearly with depth. Figure 13 is the velocity logs of Da 001 and Te 001 wells located in the south western and east central portion of block A. Only one formation in Da-001 well has velocity increase approximately with depth, while in Te-001 well, two formations has velocity increase linearly with depth. The average residual/error increases with depth as observed in Kerri-Kerri (-136.44m) and Gongila (1101.35 m) Formations (Table 3).

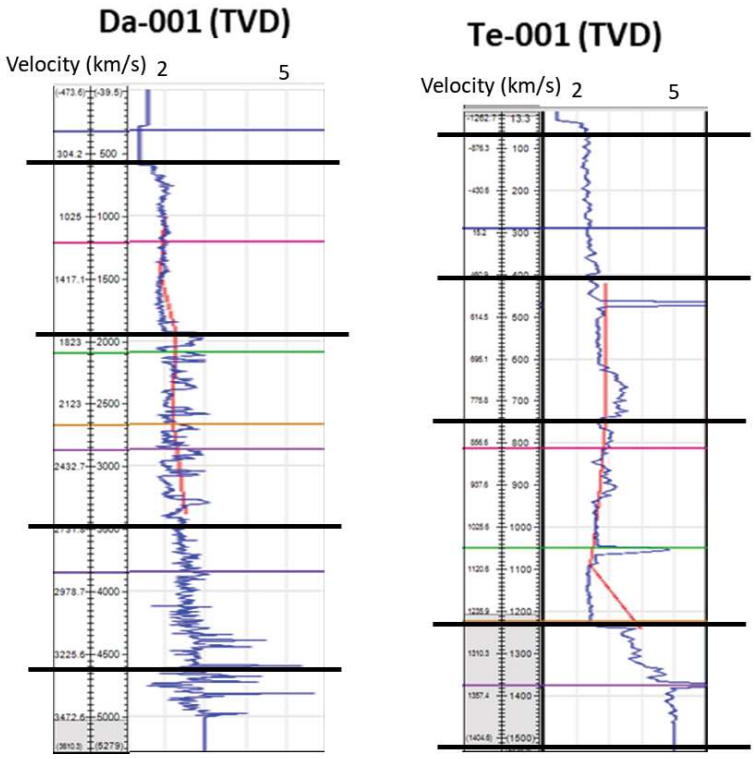


Figure 13: Portion of Velocity log across several formations

3.2 Discussions

A single time-depth function each was derived and used for 2nd Order Polynomial and V_0k+Z techniques for depth conversion from which the structure maps were estimated. Kerri-Kerri Formation representing the shallow levels was penetrated by all the wells at a depth range of -470.53 and -970.34 meters while Gongila Formation was tested at a deeper geologic section with depth rage of -1077.15 and -2837.69 meters. The overburden appeared to be structurally modest, a similar compaction trend and gentle uplift at the south-western portion of the research area, signifying the feasibility of the three techniques. Compared with the time structure maps of the two formations, the depth-converted structure maps using the three techniques shows no disparities in shape but the structure appeared fairly broad in geometry at the western part of the block on both levels. Hence, we did not consider lateral velocity differences (Figures 14 and 15).

A quantitative assessment of the depth residual values (errors) calculated at the well control points is tabulated in Table 1-4. The statistical analysis of the three velocity models adopted for Kerri-Kerri and Gongila Formations in this study shows that each model has a degree of

accuracy in depth conversion at well control of the two formation tops. Using the average velocity technique, the converted depth structure maps appeared to be the most optimal method as it gives the least average residual of -0.12 m and 1.45 m at both Kerri-Kerri and Gongila Formations. The average percentage error/residual of 0.038 and 0.023 were recorded in Kerri-Kerri and Gongila Formations respectively (Table 1). The 2nd Order Polynomial Time- Depth Analytical Function for the same formations gives residual values of -250.6 and 1,516.25 meters respectively with percentage error between 1% and 24% (Table 2). The Instantaneous Velocity Analytical Function gives residual values of -136.44 and 1,101.35 meters respectively and percentage residual range of 0.5% and 29% (Table 3).

GALLEY PROOF

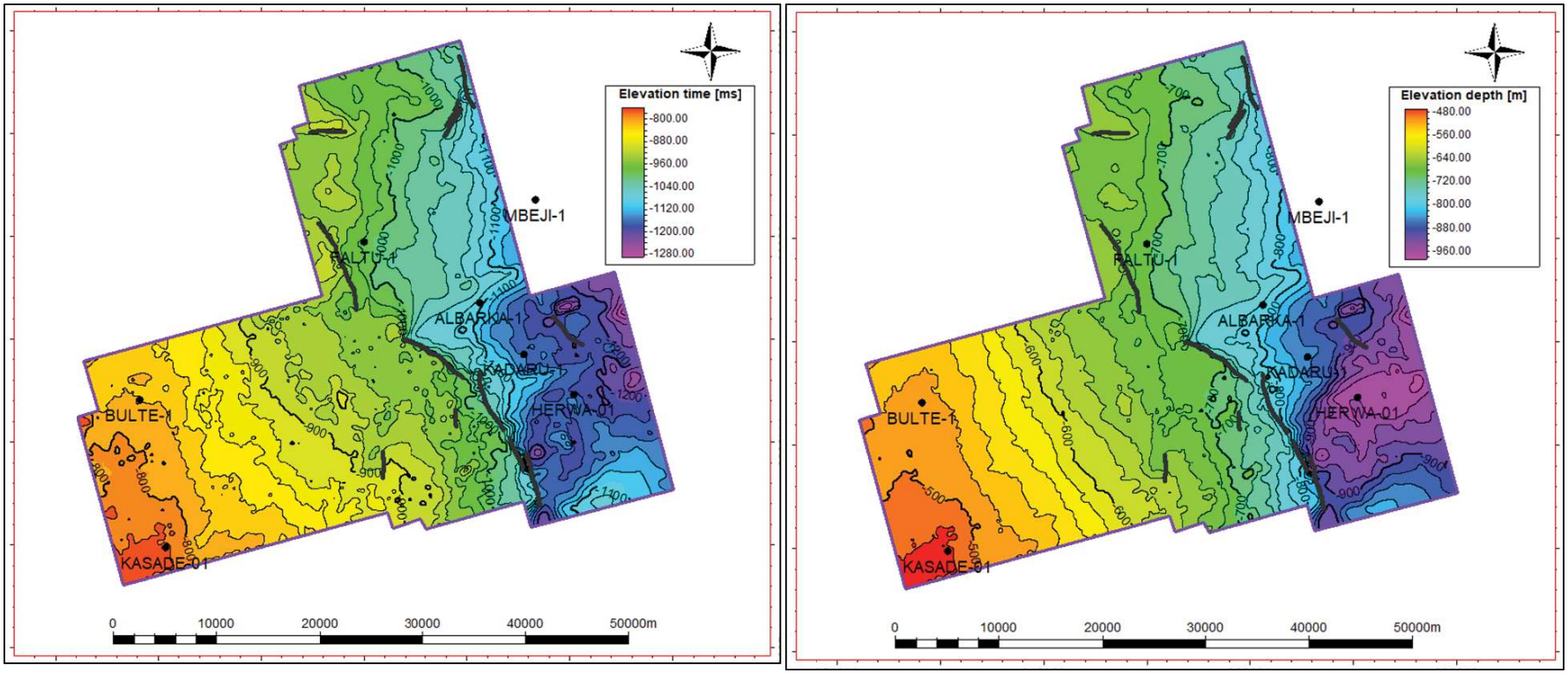


Figure 14a: Time structure map of Kerri-Kerri Fm. 14b: Depth structure map of Kerri Kerri Fm using Average Velocity function

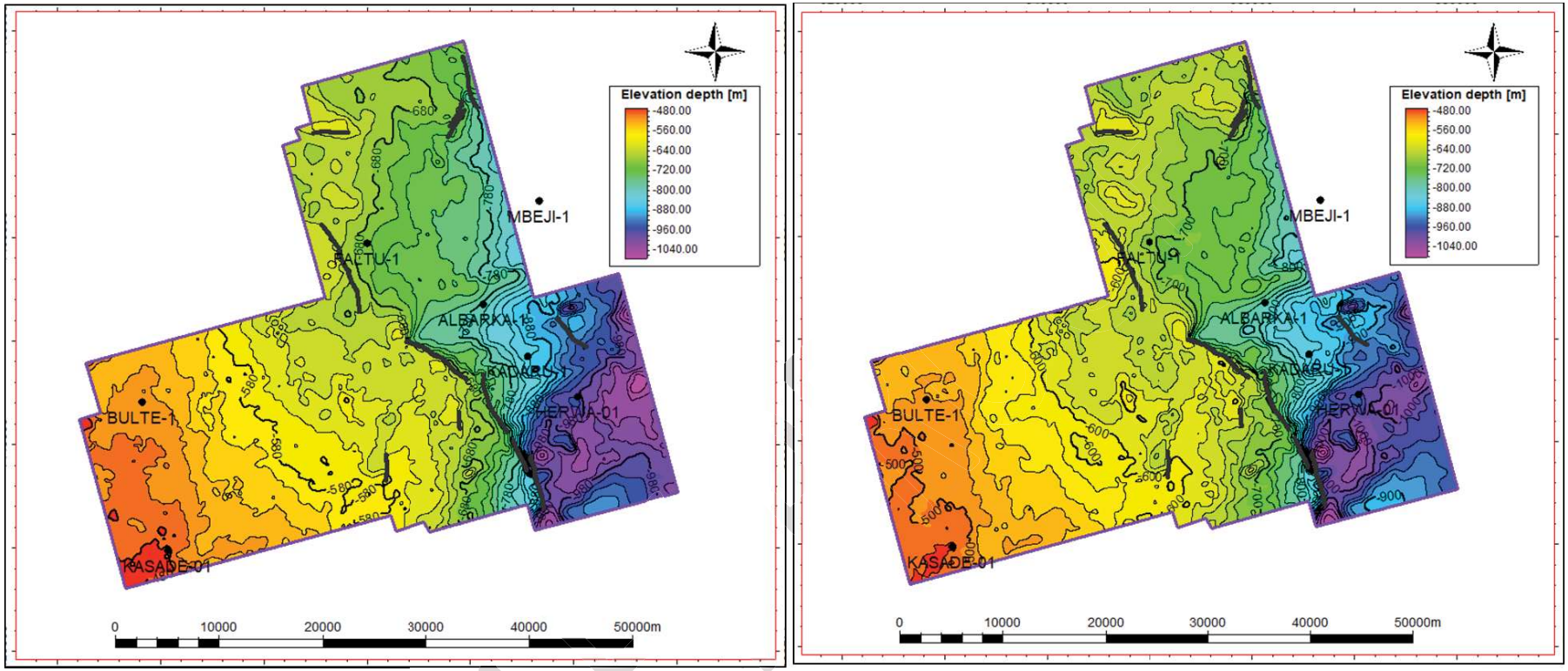


Figure 14c: Depth structure map of Kerri-Kerri Fm. Using using 2nd Order Polynomial function. 14d: Depth structure map of Kerri Kerri Fm. using instantaneous velocity function.

GALLEY

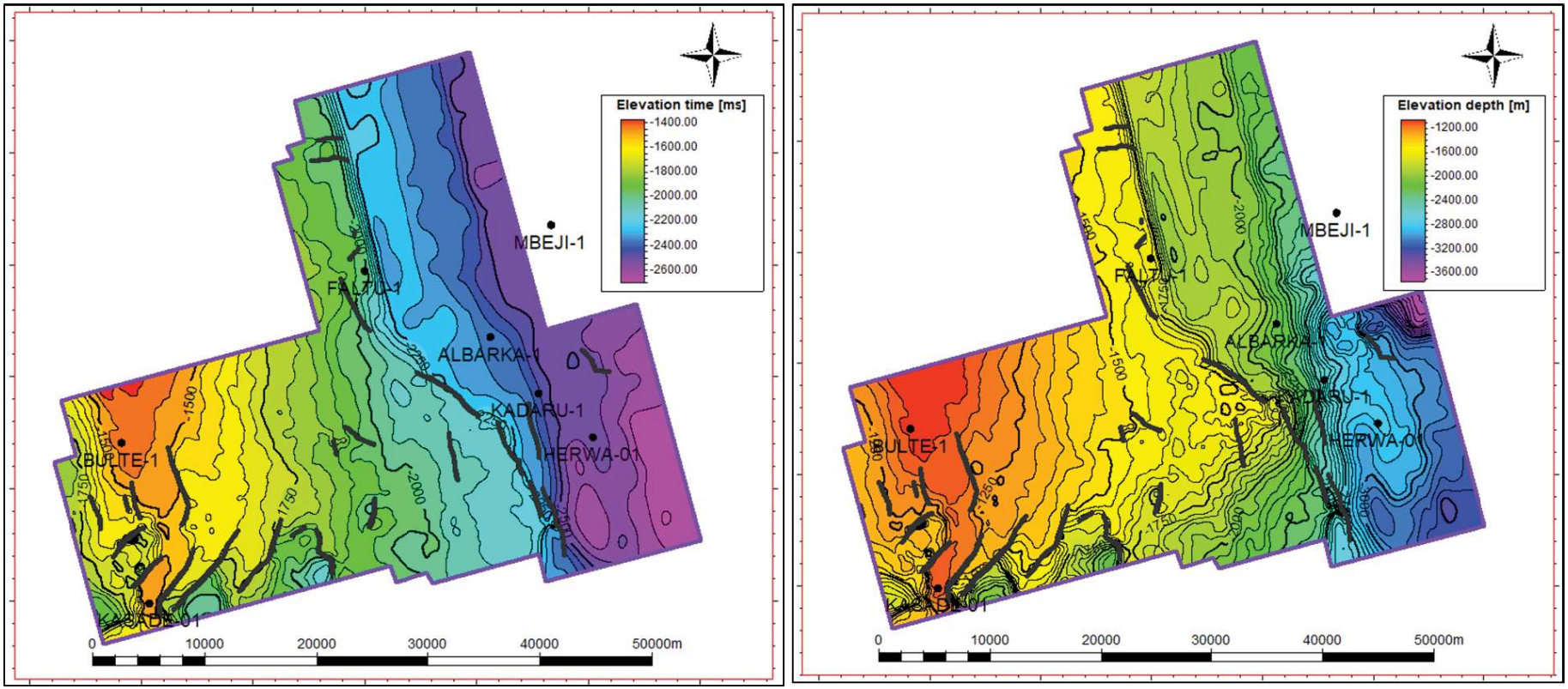


Figure 15a: Time structure map of Gongila Fm. 15b: Depth structure map of Gongila Fm using Average Velocity function.

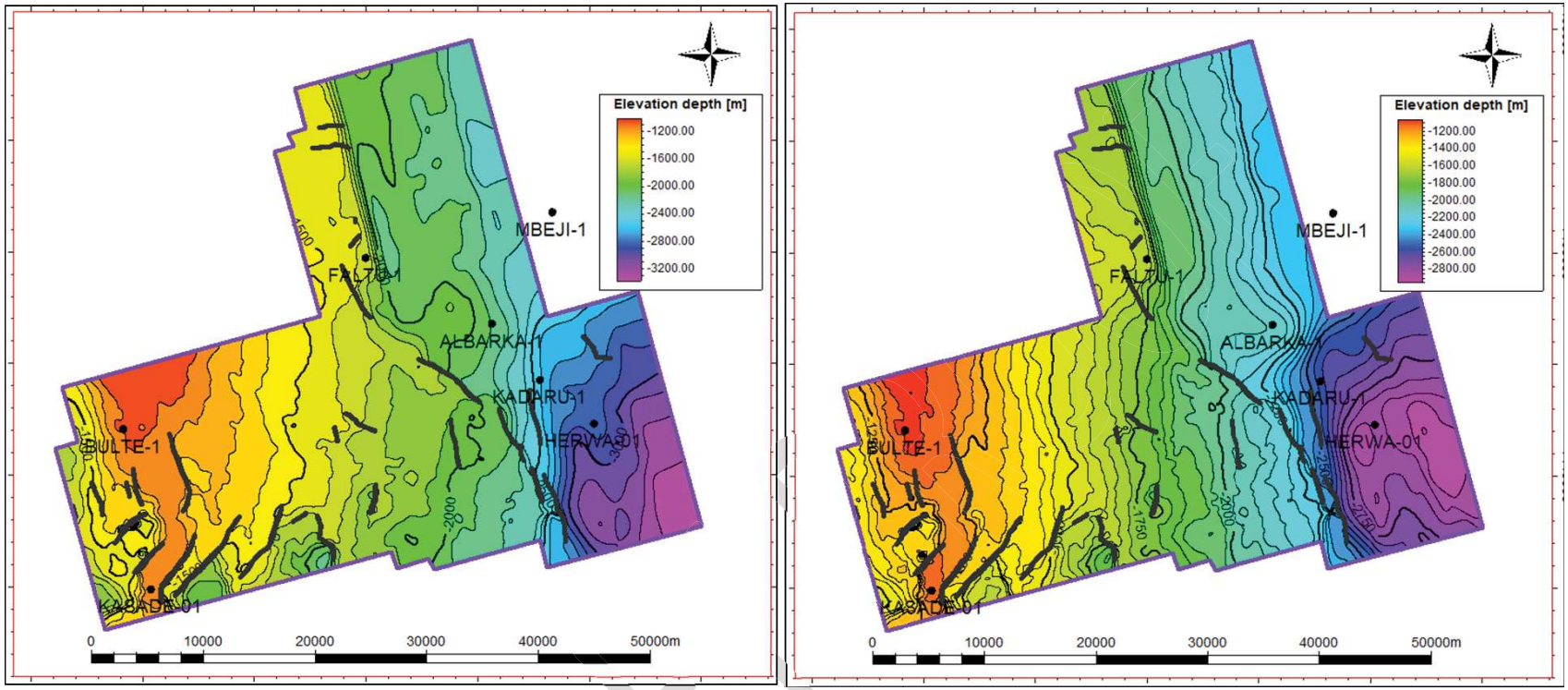


Figure 15c: Depth structure map of Gongila Fm. Using using 2nd Order Polynomial function. 15d: Depth structure map of Gongila Fm. using instantaneous velocity function.

GALLEY

4.0 Conclusions

In most practical circumstances, residual or error of less than 5% could be regarded as acceptable threshold in predicting formation depth. The three methods of depth conversion used in this study are: average velocity-time analytical function, 2nd order polynomial time-depth analytical function and instantaneous velocity analytical function. Of the three techniques tested, it is evident that the average velocity-time analytical function method appeared to be more reliable as it gives the least average residual of -0.12 m and 1.45 m at both Kerri-Kerri and Gongila Formations with average percentage error/residual of 0.038 and 0.023 recorded in the two formations. This method was therefore recommended for velocity modeling and depth conversion in Baga/Lake sub-basin of Borno Basin Nigeria. The uncertainty in depth conversion is very high using V_0-K technique with percentage error of between 0.5% and 29%, while the percentage error recorded using second order polynomial method is between 1% and 24%. The high residual documented could be as a result of using a single velocity-depth function over the whole overburden.

References

Adegoke O.S., Agamanu A.E, Benkhelil M.J. and Ajayi P.O 1986. New Stratigraphic, Sedimentologic and Structural data on Keri-Keri Formation, Bauchi Borno State Nigeria. J. Afr. Earth Sci., 5(3)249-277.

Adekoya John Adeyinka, Ola Peter Sunday and Olabode Solomon Ojo, 2014. Possible Borno Basin Hydrocarbon Habitat- A Review. International Journal of Geosciences. **5**, 983-996

Al-Chalabi, M., 1994.Seismic velocities - a critique, First Break, 12, no. 12, 589-596.

Al-Chalabi, M., 1997. Time-depth relationships for multilayerdepth conversion: Geophysical Prospecting, 45,715–720, doi: 10.1046/j.1365-2478.1997.520293.x.

Al-Chalabi, M., 1997b. Parameter nonuniqueness in Velocity versus depth functions: Geophysics, Volume 62, No 3; P. 970-979

Al-Chalabi, M., 2014. Principles of seismic velocities andtime-to-depth conversion: EAGE Publications.

Amery G. B., 1993.Basics of seismic velocities, Geophysics: The leading Edge of Exploration Pgs. 1087-1091

Avbovbo, A. A., Ayoola, E. O., & Osahon, G. A., 1986. Depositional and structural styles in Chad basin of Northeastern Nigeria. American Association of Petroleum Geologist Bulletin, 70(12),

Carter M. D., 1989. Depth conversion using normalized interval velocities. Geophysics: The Leading Edge of exploration pgs. 15-16

Etris E.L., Crabtree N.J., and Dewar J. 2002. True Depth Conversion: More Than a Pretty Picture: Scott Pickford, A Core Laboratories Company Vol. 26 No 09

Genik G., J., 1992. Regional framework, structural and petroleum aspects of rift basins in Niger, Chad and Central African Republic (C.A.R.). Tectonophysics 213: 169-185.

Genik G., J., 1993. Petroleum geology of cretaceous-tertiary rift basins in Niger, Chad and Central African Republic. AAPG Bull 77: 1405-1434

Guiraud, M., 1990. Tectono-sedimentary framework of the early Cretaceous continental Bima Formation (Upper Benue trough, NE Nigeria). Journal of African Earth Sciences, 10(1/2):341-353.

Guiraud, M. 1991.Mécanisme de formation du basin Crétacé sur décrochements multiples de la Haute-Bénoué (Nigéria). *Bull. Centres Rech. Explor-Prod. Elf-Aquitaine*, 15(1):1-67.

Keho T. and Samsu D., 2002. Depth conversion of Tangguh gas fields. Geophysics: The Leading Edge of Exploration pgs. 966-971.

Krehbiel S., 1993. Depth estimates of seismic reflection data in SW Washington, Geophysics: The Leading Edge of Exploration pgs. 1076-1081

Marsden, D., 1992. Vo-K method of depth conversion, Geophysics: The Leading Edge of Exploration, p. 53-54.

GALLEY PROOF

Marsden, D., Bush M. D., and Johng D. S., 1995.Analytical velocity functions, Geophysics: The Leading Edge of Exploration, p. 53-54.

Moumouni, A., Obaje. N.G, Nzegbuna, A.I and Chaana, M.S 2007. Bulk Geochemical Parameters and Biomarker Characteristics of Organic Matter in Two Wells (Gaibu-1 and Kasade-1) from the Bornu Basin: Implication on Hydrocarbon Potentials. Journal of Pet. Sci. and Engr. 58, 275 – 282

Obaje N.G., Wehner H, Scheeder G, Abubakar MB, Jauro A 2004a. Hydrocarbon prospectivity of Nigeria's inland basins: From the viewpoint of organic geochemistry and organic petrology. AAPG Bulletin 87: 325-353.

Okosun E.A., 1995. Review of the geology of Bornu Basin. Jornal of Min Geo 31: 113- 122.

Ola P.S., Adekoya J.A., Olabode S.O., 2017. Source Rock Evaluation in the Lake Chad Area of the Bornu Basin, Nigeria. J Pet Environ Biotechnol 8: 346. doi: 10.4172/2157-7463.1000346

Olugbemiro R.O., Ligouis B., and Abaa S.I., 1997. The Cretaceous series in the Chad Basin, NE Nigeria source rock potential and thermal maturity. J Pet Geo 20: 51-58.

Onuoha, K.M. 1999. Structural Features of Nigeria's Coastal Margin: An Assessment Based on Age Data from Wells. Journal of African Earth Sciences, **29**, 485-499. http://dx.doi.org/10.1016/S0899-5362(99)00111-6

Omolaiye G.E., Ayolabi E. A., and Ololade I., 2011. Velocity trends analysis of compacted clastic rocks of Efomeh field, Onshore Niger Delta, Nigeria. Journal of sci. Res. Dev. Vol 13, 37-47.

Sava, P., and B. Biondi, 2004, Wave-equation migration velocity analysis. I: Theory: Geophysical Prospecting, 52, 593–606, doi: 10.1111/j.1365-2478.2004.00447.x.

Schultz, P., 1999.The Seismic Velocity Model as an Interpretation Asset, 1999 Distinguished Instructor Short Course, Distinguished Instructor Series, No. 2, SEG.

Slotnick, M. M., 1936. On seismic computation with applications. Geophysics, 1, 9-22.

Syukri, I.Y., Hughes, J., and Medianesterian, M., 2014. Comparison of depth conversion methods in Buntal Gas Field, Block B, Natuna Sea Indonesia. Preceding Indonesian Petroleum Association 38th Annual Conference and Exhibition.

Velásquez A. J., and Alfonso H. 2018.Depth-conversion techniques and challenges in complex area.

GAP PROOF

List of Tables

Table 1a: Residual values obtained using average velocity depth converted maps on Kerri-Kerri Formation Top

Well	Measure Depth	Z-value	Horizon before	Error	Horizon after	% Error
Da-001	1143.99	-854.97	-916.73	1.24	-854.97	-0.15
Ft-001	999.09	-692.37	-693.72	1.35	-692.37	-0.19
Ak-001	1089.17	-782.46	-782.93	0.47	-782.46	-0.06
Sa-001	768.84	-470.53	-472.02	1.5	-470.53	-0.32
Wa-001	1262.16	-970.34	-965.69	-4.65	-970.34	0.48
Te-001	812.14	-515.53	-515.5	-0.03	-515.53	0.01

Table 1b: Residual values obtained using average velocity depth converted maps on Gongila Formation Top

Well	Measure Depth	Z-value	Horizon before	Error	Horizon after	% Error
Da-001	1942.17	-1635.44	-1634.63	-0.81	-1635.44	0.05
Ft-001	1373.78	-1077.15	-1077.78	0.62	-1077.15	-0.06
Ak-001	2414.55	-2107.82	-2107.75	-0.07	-2107.82	0.00
Sa-001	1429.69	-1131.36	-1132.62	1.26	-1131.36	-0.11
Wa-001	2868.63	-2579.60	-2581.05	1.45	-2579.60	-0.06
Te-001	3129.53	-2837.69	-2836.69	-1	-2837.69	0.04

Table 2a: Residual values obtained using polynomial function converted maps on Kerri-Kerri Formation Top

Well	Measure Depth	Z-value	Horizon before	Error	Horizon after	% Error
Da-001	1143.99	-854.97	-862.85	7.88	-854.97	-0.92
Ft-001	999.09	-692.37	-648.79	-43.58	-692.37	6.29
Ak-001	1089.17	-782.46	-772.73	-9.73	-782.46	1.24
Sa-001	768.84	-470.53	-407.17	-63.35	-470.53	13.46
Wa-001	1262.16	-970.34	-880.92	-89.43	-970.34	9.22
Te-001	812.14	-515.53	-463.13	-52.39	-515.53	10.16

Table 2b: Residual values obtained using polynomial function converted maps on Gongila Formation Top

Well	Measure Depth	Z-value	Horizon before	Error	Horizon after	% Error
FALTU-1	1942.17	-1635.44	-2029.51	394.06	-1635.44	-24.10
BULTE-1	1373.78	-1077.15	-1189.46	112.31	-1077.15	-10.43
ALBARKA-1	2414.55	-2107.82	-2680.24	572.43	-2107.82	-27.16
KASADE-01	1429.69	-1131.36	-1266.73	135.37	-1131.36	-11.97
KADARU-1	2868.63	-2579.60	-2797.03	217.43	-2579.60	-8.43
HERWA-01	3129.53	-2837.69	-2922.34	84.65	-2837.69	-2.98

Table 3a: Residual values obtained using instantaneous velocity model depth converted maps on Kerri-Kerri Formation Top

Well	Measure Depth	Z-value	Horizon before	Error	Horizon after	% Error
Da-001	1143.99	-854.97	-838.76	-16.21	-854.97	1.90
Ft-001	999.09	-692.37	-710.43	18.06	-692.37	-2.61
Ak-001	1089.17	-782.46	-786.27	3.81	-782.46	-0.49
Sa-001	768.84	-470.53	-374.64	-95.89	-470.53	20.38
Wa-001	1262.16	-970.34	-992.82	22.48	-970.34	-2.32
Te-001	812.14	-515.53	-446.84	-68.69	-515.53	13.32

Table 3b: Residual values obtained using instantaneous velocity model depth converted maps on Gongila Formation Top

Well	Measure Depth	Z-value	Horizon before	Error	Horizon after	% Error
Da-001	1942.17	-1635.44	-1881.57	246.13	-1635.44	-15.05
Ft-001	1373.78	-1077.15	-1037.08	-40.08	-1077.15	3.72
Ak-001	2414.55	-2107.82	-2726.40	618.59	-2107.82	-29.35
Sa-001	1429.69	-1131.36	-1180.81	49.45	-1131.36	-4.37
Wa-001	2868.63	-2579.60	-2758.02	178.42	-2579.60	-6.92
Te-001	3129.53	-2837.69	-2886.53	48.84	-2837.69	-1.72

Table 4: Comparing the Residual values obtained in the three methods

Methodology	Kerri-Kerri Formation	Gongila Formation
Average Velocity-Time Analytical Function	-0.12 meters	1.45 meters
2nd Order Polynomial Time-Depth Analytical Function	-250.6 meters	1,516.25 meters
Instantaneous Velocity Analytical Function	-136.44 meters	1,101.35 meters